Diffusion-controlled reactions in small and structured spaces as a tool for describing living cell biochemistry

2007 J. Phys.: Condens. Matter 19 065149

(http://iopscience.iop.org/0953-8984/19/6/065149)

INSTITUTE OF PHYSICS PUBLISHING JOURNAL OF PHYSICS: CONDENSED MATTER

J. Phys.: Condens. Matter **19** (2007) 065149 (12pp) doi:10.1088/0953-8984/19/6/065149

Diffusion-controlled reactions in small and structured spaces as a tool for describing living cell biochemistry

Z Konkoli

Department of Applied Physics, Chalmers University of Technology, SE-41296 Göteborg, Sweden

E-mail: zorank@fy.chalmers.se

Received 27 July 2006, in final form 25 September 2006
Published 22 January 2007
Online at stacks.iop.org/JPhysCM/19/065149

Abstract

A simplified model of the living cell is studied. The reaction space is divided into compartments and the structured (non-compact) geometry is described in terms of a network consisting of containers connected by tubes. By assumption, reactions in the containers (tubes) are allowed (forbidden). It is assumed that the number of reactants is low, leading to stochastic (noisy) dynamics. By varying the transport rate among various containers D relative to the reaction rate within each container λ, using either $D \gg \lambda$ or $D \ll \lambda$, a transition from a reaction-controlled (reactants mix well) towards a diffusion-controlled (large spatial fluctuations) regime can be studied. The focus is on a study of the timing of chemical reactions. For a single set of chemical reactions, the reaction times $\boldsymbol{t} = (t_1, t_2, \ldots)$ are defined as the time intervals needed to synthesize a given amount of molecules (of various types and in different regions of the system). The components of $\boldsymbol{t}$ are stochastic (non-independent) variables described in terms of two moments: average $\boldsymbol{\tau} = (\tau_1, \tau_2, \ldots)$ and standard deviation $\boldsymbol{\sigma} = (\sigma_1, \sigma_2, \ldots)$. In such a way it is possible to have a measure of the reaction speed ($\boldsymbol{\tau}$) and noise content ($\boldsymbol{\sigma}$). A large number of chemical reactions were classified by monitoring how norms τ and σ vary as the geometry of the system changes from compact (τ_0, σ_0) towards structured (τ_n, σ_n). It is found that there are reactions that draw benefits in terms of both increased reaction speed ($\tau_n < \tau_0$) and noise reduction ($\sigma_n < \sigma_0$). Such reactions become faster and synchronize better in structured space. There are reactions that exhibit an increase in speed ($\tau_n < \tau_0$) but become more noisy and harder to synchronize ($\sigma_n > \sigma_0$). Opposite cases are possible where reactions become slower ($\tau_n > \tau_0$) but more accurate ($\sigma_n < \sigma_0$).

1. Introduction

Diffusion-controlled reactions are ubiquitous in nature and have been explored intensively over a long time period. The simplest way to define diffusion-controlled reactions is by using a lattice model in which reactants move on the lattice with a jump rate D and when meeting at

the same lattice site react with a reaction rate λ. An interesting situation arises when $\lambda \gg D$: diffusion does not mix the reactants well and large spatial fluctuations develop. Any attempt to describe such kind of kinetics using mean field theory fails. This kind of dynamics is normally referred to as *anomalous* (non-mean field), or *fluctuation dominated*. Numerous experimental and theoretical investigations have been devoted to these problems (e.g. see [1–7] for reviews on the subject).

The theoretical investigation of diffusion-controlled reactions is still a very active field. There are a couple of reasons for this. First, even in traditional settings (large volumes, point reactants) the field is extremely technical. An enormous number of computational methods have been developed to describe diffusion-controlled reactions but none of them gives a definite answer. There is still a large challenge on the method development front that has to be overcome since each new problem requires its own set of approximations. Second, novel phenomena are investigated that give an additional boost to the field. One example is the study of diffusion-controlled reactions in liposome networks. A review of this work is given in [8].

Out of numerous studies of diffusion-controlled reactions the investigations of diffusion-controlled reactions in restricted geometries might be the one that is most relevant to this paper. When the size of the reaction volume is slightly larger than the typical size of reactants, new phenomena arise. For example, due to the presence of geometrical constraints, exclusion effects become important. Low particle numbers lead to the fact that the dynamics becomes noisy. Also, chemical details have to be accounted for. Steric effects start showing up: the reactants cannot be described as uniform reacting spheres, but have reactive spots, and have to approach each other in a specific way in order to react. These phenomena have been explored in a large number of studies. Some work can be found in [9–18].

In this work the focus is on the investigation of diffusion-controlled reactions in environments reminiscent of the ones found in the living cell. Due to the small cell size the diffusion is frequently employed as a transport mechanism. There are other means of transport such as the ones that use motor proteins, but diffusion is often employed. For example, for a cell of the size $L \sim 1\ \mu$m and diffusion constant of regulatory molecules of the order $D_r \sim 10^{-6}$–10^{-5} cm^2 s^{-1}, one gets a mixing time of the order $t_{mix} \sim L^2/D_r \sim$ 1–10 ms [19]. Due to the frequent use of diffusion in the living cell dynamics the tools being developed to study diffusion-controlled reactions in general, and reactions in restricted geometries in particular, could prove extremely useful.

Modern research in cytology shows that chemical reaction dynamics in the cell interior cannot be described in the framework of bulk studies (for a review on the subject see [20–23]). A living cell interior is *structured*: the space is divided into various regions. Part of the intracellular space is taken by organelles such as Golgi apparatus or mitochondria. Even the region outside organelles is not smooth, being crowded with obstacles. In the cell interior, the concentration of macromolecules can be as high as 30% by weight [22]. In such an environment the reactants do not have much space to move, and the motion of individual molecules is heavily influenced either by other molecules that move around (and possibly react with them) or by static obstacles that are present. In addition, the geometrical arrangement of reactants can be quite complicated. There are few examples of protein complexes that are closely packed in careful geometrical arrangement in order to carry out synthesis [24, 23]. Also, reaction volumes can be quite dynamic: protein complexes are formed just in order to execute (catalyse) chemical reactions and they disappear once the synthesis is done [24].

The assumption that the cell interior is a smooth, compact, and static space is simply incorrect, and there is experimental evidence for that. In this context it is natural to wonder about the role of diffusion-controlled reactions. To what extent should we revise what we know about these reactions in order to be able to describe living cell biochemistry? New

unifying concepts might be needed to understand such an environment. In this paper some issues related to the kinetics of diffusion-controlled reactions in small and structured geometries will be addressed. A framework is presented that can be used to study the timing of chemical reactions in structured (and dynamic) spaces such as the ones found in the living cell.

A large number of studies have dealt with describing various issues of timing in the cell biochemistry. For example, a living cell avoids unnecessary storage of chemicals by carefully scheduling reaction events. Reactants are transported to various parts of the cell exactly at the time and place that they are needed. Large numbers of studies have explored these issues [19, 25–31]. The inspiration for the present work comes from investigations.

When the number of reactants is low the dynamics is stochastic and noisy. In such a case the exact arrival of chemicals cannot be precisely defined. It is exactly such a situation that is investigated in this work. Accuracy in timing is important if reactions are to function in synchronous mode. A large number of chemical reactions will be studied and they will be classified with regard to the noise characteristics they posses. Previously, a similar study was done in which the focus was on the average time for reactions to complete [32].

The details of the chemical reactions and transport are omitted. The reactants are assumed to be point-like objects and only three scales are kept in the problem: the reaction rate λ, the transport rate D, and the parameter ξ that describes catalytic influences. Also, a rather crude approximation of living cell geometry is made. The details of the geometry of the living cell and organelles it contains do play a role [33–35]. However, here the geometry is greatly simplified. An attempt will be made to model the fact that the cell interior is not a large open space but is divided into many regions.

Figure 1 shows a schematic presentation of what is being studied. Panels (a)–(c) depict three different ways of modelling the chemical reaction dynamics of the living cell. In the first approximation one can think of a cell as a closed space that harbours a certain amount of reactants, as shown in panel (a). The reactants freely move around since there are no obstacles (apart from the fact that they influence each other through exclusion effects). Panel (b) shows the situation where space is structured and the mixing of reactants is not as efficient as in the previous case depicted in panel (a). Panel (c) shows how complicated space in panel (b) is modelled in terms of simple geometrical objects (spheres and tubes connecting them).

Panel (c) lacks all the details of panel (b) but it does capture the most important aspects of the problem. The simplified version of the structured space depicted in panel (c) is easier to address theoretically. Also, the structures depicted in panel (c) can be routinely built in the laboratory as liposome networks. The experimental details can be found in work published in [36]. The motivation to use the setup presented in panel (c) as a model of structured space comes from [36].

How do we investigate the changes in reaction dynamics when the geometry is altered from compact (panel (a)) towards structured (panel (b))? Such a transformation would be hard to describe in mathematical terms and another more practical route has to be followed. In the following the focus will be on panel (c). The transition from panel (a) to panel (b) can be simulated by increasing the lengths of the tubes in panel (c). When the tubes are short one has compact geometry (e.g. the one depicted in panel (a)); when they are long one has structured geometry (as in panel (b)). Equivalently, instead of physically changing the tube lengths only the transport rate D will be altered. One simply has to study changes in reaction timing as the transport rate changes from $D \gg \lambda$ (reaction controlled) towards $D \ll \lambda$ (diffusion controlled). This is the main idea of the paper[1].

[1] The classical field of fluctuation-dominated kinetics can be seen as a special case of the setup studied here in which the network used is regular, with a well defined number of neighbours.

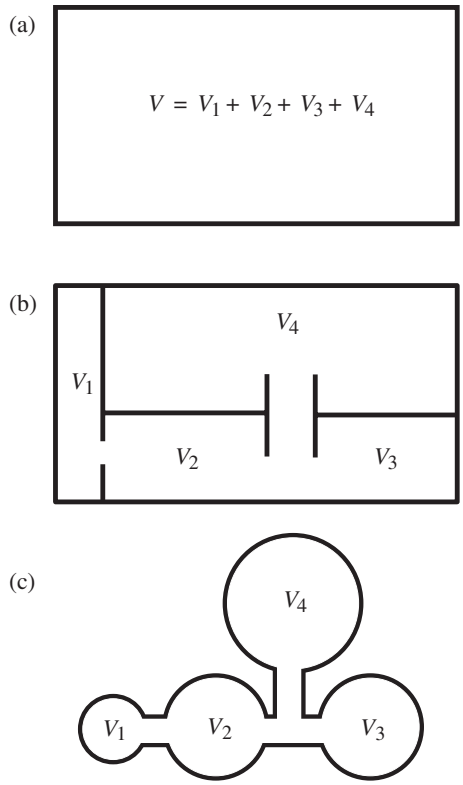

Figure 1. The goal is to understand how the reaction dynamics alters when the geometry of the system changes from compact, shown in panel (a), towards non-compact (structured), shown in panels (b) and (c). Panel (a) rough model of the cell in which reactants move inside a close volume. Panel (b) a more realistic model of the living cell showing that it is structured. Panel (c) a network consisting of containers and tubes is used to capture the most important geometrical features of the problem. For example, the drawing in panel (c) reflects the relative size of the volumes in panel (b): $V_1 < V_2 \approx V_3 < V_4$. The connectivity patterns in (b) and (c) are the same. Varying length of the tubes can be accounted for by adjusting the corresponding transport coefficients (however, for simplicity reasons, only one parameter D is used). When $D \ll \lambda$ the reaction dynamics in panels (b) and (c) should exhibit some similarities. For $D \gg \lambda$ one expects the same for the structures (a) and (c).

The paper is organized as follows. In section 2 the dynamics is defined with all necessary details. Section 3 describes how reaction times are defined, and is one of the most important building blocks of the paper. Section 4 explains how various chemical reactions are compared and classified. The most important results of this paper are discussed in section 5.

2. Definition of dynamics

The model introduced in a previous study [32] is used. Here, only a brief summary of the model will be given, since all details can be found in the previous publication. By assumption, the particles move in the network depicted in figure 1 (panel (c)). The transport rate is given by D provided there is a link between containers. If particles are allowed to react, they do this within containers with rate λ. Reactions in tubes are not allowed. In such a way the transport scale and reaction scales are clearly separated.

For computational convenience a very simple type of reaction scheme will be considered:

$$X_\alpha \overset{\pm X_\gamma}{\rightarrow} X_\beta \tag{1}$$

where $+X_\gamma$ ($-X_\gamma$) implies that the X_γ molecule is a promoter (inhibitor) for the reaction modifying the bare reaction rate λ into $\xi\lambda$ (λ/ξ). Variable $\xi \gg 1$ denotes the catalysis enhancement factor and it is taken very large in order to amplify the catalytic influences. Symbol X_γ is omitted if the reaction is not catalysed.

To describe the system at any time instant it is sufficient to track the number of particles in each container. The state of the system is specified by vector $\boldsymbol{c}$, where

$$\boldsymbol{c} = [\boldsymbol{n}_1; \ldots; \boldsymbol{n}_i; \ldots; \boldsymbol{n}_N] \tag{2}$$

and

$$\boldsymbol{n}_i = (n_{1,i}, \ldots, n_{\alpha,i}, \ldots, n_{M,i}). \tag{3}$$

For example, $n_{\alpha,i}$ is a variable that specifies the number of X_α molecules in container C_i. The dynamics of $\boldsymbol{c}$ is governed by the master equation

$$\dot{p}(\boldsymbol{c}, t) = \sum_{\boldsymbol{c}'} R_{\boldsymbol{c},\boldsymbol{c}'}\, p(\boldsymbol{c}', t) - \sum_{\boldsymbol{c}'} R_{\boldsymbol{c}'\boldsymbol{c}} p(\boldsymbol{c}, t). \tag{4}$$

A dot over a symbol denotes time derivative and $p(\boldsymbol{c}, t)$ specifies occupation probabilities. The reaction rates $R_{\boldsymbol{c}'\boldsymbol{c}}$ for the $\boldsymbol{c} \rightarrow \boldsymbol{c}'$ transition can be easily calculated from the details of how the reaction rates are defined.

3. Defining reaction time

The goal is to compare various reactions with regard to reaction time. In order to be able to define the reaction time one has to fully specify the initial condition and when the dynamics ends. This is done through the use of inject and task patterns $\boldsymbol{\iota}$ and $\boldsymbol{\pi}$. First, one has to define how the dynamics starts: $\boldsymbol{\iota} = \boldsymbol{c}(0)$. Second, the dynamics stops when molecules are synthesized for the first time. The end of the reaction cycle is defined by specifying the type of molecules that needs to be synthesized, their amount, and in which container. This information is embedded in vector $\boldsymbol{\pi}$.

Task pattern $\boldsymbol{\pi}$ does not specify the configuration of the system in the strict sense as $\boldsymbol{c}$ and $\boldsymbol{\iota}$ do. As an illustration a simplest non-trivial network with two containers C_1 and C_2 connected by the tube will be discussed. This network is depicted in figure 2. For example, the dynamics can be started from configuration $\boldsymbol{\iota} = [(2A, 1B); (0A, 1B)]$[2]. Also, in the case of two containers it is convenient to use slightly different notation and denote the inject pattern as $\boldsymbol{\iota} = [2A, 1B] - [1B]$. Task patterns will be indicated in similar way. For example, it could be specified as $\boldsymbol{\pi} = [3A] - [1A, 2B]$. This expression does not indicate that the dynamics stops when configuration $\boldsymbol{c} = [3A, 0B); (1A, 2B)]$ is reached![3] Instead, the following interpretation is used. There are three (sub)tasks that need to be achieved. π_1: three A molecules have to be synthesized in container C_1 (the amount of B molecules in this container is not monitored); π_2: one A molecule has to be synthesized in C_2; π_3: two B molecules have to be synthesized in C_2. This can happen in arbitrary order. Depending on the reaction scheme it might happen that some subtasks are never realized, and such a possibility is allowed. In such a way, there is a large amount of flexibility when individual molecules are delivered. It might happen that they all arrive at the same time, but we are not requiring this to happen.

[2] This implies that at $t = 0$ two A molecules and one B molecule are inserted in C_1, and only one B molecule in container C_2.

[3] In the real cell it is extremely unlikely that a large number of molecules will be delivered at the same time. Such a system would very likely be unstable and prone to errors and, accordingly, such a scenario is not explored here.

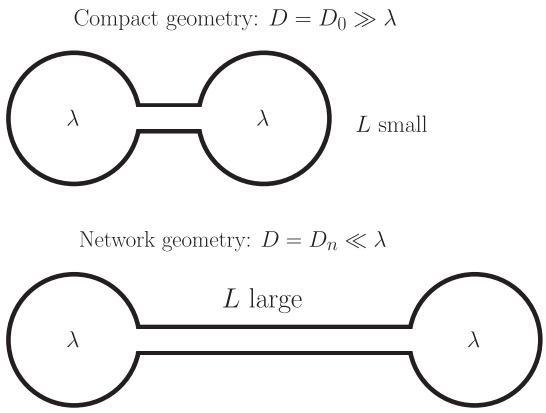

Figure 2. Simplest case of structured geometry: two volumes connected by a tube of length L. Changes in average reaction time and its standard deviation when going from network like (stretched) towards compact geometry are embedded in two parameters ν_τ and ν_σ.

Thus, $\boldsymbol{\pi} = [3A] - [1A, 2B]$ specifies that three subtasks are monitored and one operates with three stochastic variables t_1, t_2 and t_3 associated with subtasks π_1, π_2, and π_3. In general, these stochastic variables are not independent since, by assumption, once a subtask is achieved the molecules that achieved it are removed from the system. The motivation for removing molecules in such a way, apart from making the model more interesting by coupling all variables, comes from analysis of the behaviour of the living cell. For example, substrate molecules are always consumed and converted into something else (this is of course not true for enzymes).

Furthermore, note that each of the subtasks can be achieved through various configurations. For example, all configurations $c = [(3A, \diamond); (\diamond, \diamond)]$ are sinks (here $\diamond$ denotes any integer starting from zero and upwards), or *window states* for achieving subtask π_1.[4] Once the system reaches any such configuration three A particles are removed from C_1, and the dynamics starts again with π_1 deleted from the list of tasks.

At this stage the reaction times are well defined. Two ways of calculating various moments of these reaction times were discussed in a previous publication [32]. The details of the calculation are not important for the present work. In brief, one has to solve a master equation, such as the one given in equation (4), with perfectly absorbing window states present. In such a setup the average reaction times $\boldsymbol{\tau}$ and associated standard deviations $\boldsymbol{\sigma}$ can be readily calculated by manipulation of matrices $\boldsymbol{R}$ (see [32] for details). For each of the subtasks in $\boldsymbol{\pi}$ one needs an entry in $\boldsymbol{\tau}$ and $\boldsymbol{\sigma}$. For example, in the case of the two-container example discussed above one has τ_1 and σ_1 (corresponding to π_1), τ_2 and σ_2 (π_2), τ_3 and σ_3 (π_3), resulting in $\boldsymbol{\tau} = (\tau_1, \tau_2, \tau_3)$ and $\boldsymbol{\sigma} = (\sigma_1, \sigma_2, \sigma_3)$.

In the following, in order to facilitate numerical comparison of $\boldsymbol{\tau}$ and $\boldsymbol{\sigma}$ symbols τ and σ will refer to the norm of corresponding vectors. For example, in the case of the particular example just discussed one has $\tau = \sqrt{\tau_1^2 + \tau_2^2 + \tau_3^2}$ and $\sigma = \sqrt{\sigma_1^2 + \sigma_2^2 + \sigma_3^2}$.

[4] Once the system arrives in a window state it never leaves.

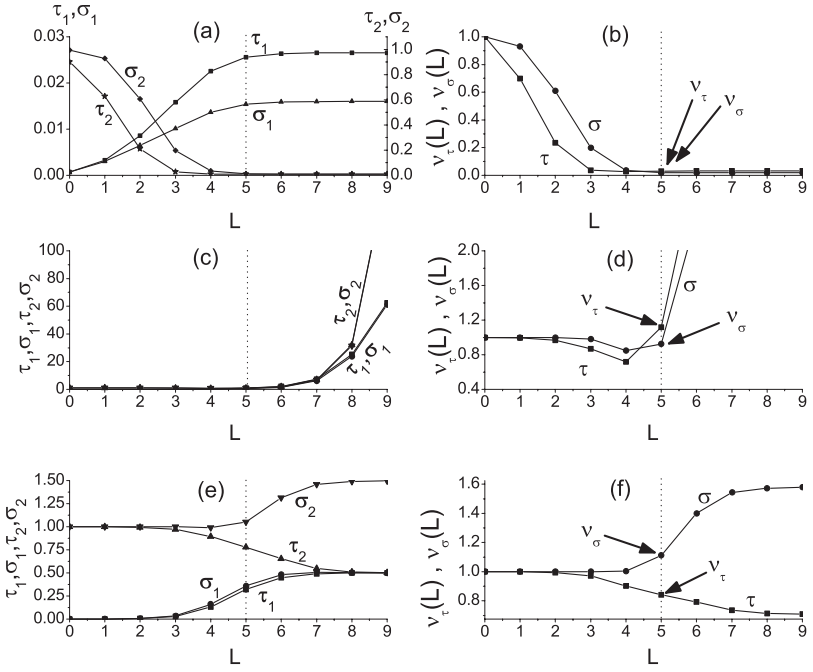

Figure 3. Dependence of τ_1, σ_1, τ_2, and σ_2 on tube length L (transport rate D); o_1: panels (a) and (b); o_2: panels (c) and (d); o_3: panels (e) and (f).

4. Comparing various chemical reactions

At this stage one is left with the hardest part of the problem. How do we compare chemical reactions that possibly involve different reaction schemes, number of particles, and are executed in different geometries?

In order to facilitate comparison of various chemical reactions in structured and compact geometries it is very useful to introduce the notion of an *artificial organism*[5]. It is defined as a triple consisting of (i) reaction scheme (specified in equation (1)), (ii) inject and task patterns $\boldsymbol{\iota}$ and $\boldsymbol{\pi}$, and finally (iii) the geometry of the problem (specified by the number of containers and connections between them). The triple harbours three essential features of the living cell: the presence of chemical reactions, intake of chemicals, and formation of products in various regions. Instead of *artificial organism* the term *organism* will be used in the following.

A few examples that will be discussed later on are as follows: organism o_1 with reaction $A \xrightarrow{+A} B$, inject pattern $\boldsymbol{\iota} = [A] - [4A]$, and task pattern $\boldsymbol{\pi} = [4A] - [B]$; organism o_2 with reaction $A \xrightarrow{-B} B$, inject pattern $\boldsymbol{\iota} = [\,] - [4A]$, and task pattern $\boldsymbol{\pi} = [3A, B] - [\,]$; and organism o_3 with reaction $A \xrightarrow{-B} B$, inject pattern $\boldsymbol{\iota} = [A] - [2A]$, and task pattern $\boldsymbol{\pi} = [2A] - [B]$. Note that the reaction is the same for o_2 and o_3. They differ in inject and task patterns and represent different organisms.

Two properties $\boldsymbol{\tau}(L)$ and $\boldsymbol{\sigma}(L)$ will be studied when the geometry varies by extending the tube length L from very short (compact geometry) towards very long (network-like geometry). Figure 3 (panels (a), (c), and (e)) is an example which shows how individual components of $\boldsymbol{\tau}$ and $\boldsymbol{\sigma}$ for o_1, o_2, and o_3 change when the tube length increases. Panels (b), (d), and (f) indicated

[5] The term *artificial cell* would be equally useful.

how the norms of $\boldsymbol{\tau}(L)$ and $\boldsymbol{\sigma}(L)$ (normalized by the value at $L = 0$) depend on tube length. In these panels two quantities are plotted, $\nu_\tau(L) = \tau(L)/\tau(0)$ and $\nu_\sigma(L) = \sigma(L)/\sigma(0)$, where $\tau(L)$ and $\sigma(L)$ denote the norm of the vectors $\boldsymbol{\tau}(L)$ and $\boldsymbol{\sigma}(L)$.

A detailed discussion on how the tube length L and exchange rate D are related can be found in [37]. Here, L is just used to label various values for D, keeping in mind that D has to decrease as L increases. By definition, $L = 0$ corresponds to $D = 3125\ \mathrm{s}^{-1}$, $L = 1$ to $D = 625\ \mathrm{s}^{-1}$, 2 to $125\ \mathrm{s}^{-1}$, 3 to $25\ \mathrm{s}^{-1}$, 4 to $5\ \mathrm{s}^{-1}$, 5 to $1\ \mathrm{s}^{-1}$, 6 to $0.1\ \mathrm{s}^{-1}$, 7 to $0.04\ \mathrm{s}^{-1}$, 8 to $0.008\ \mathrm{s}^{-1}$, and $L = 9$ to $D = 0.0016\ \mathrm{s}^{-1}$. λ is always set equal to $1\ \mathrm{s}^{-1}$.

It can be seen that o_1 draws benefit from the network-like geometry in terms of reducing both the average reaction time and the noise content, since in panel (b) $\nu_\tau(L)$ and $\nu_\sigma(L)$ decrease as L increases. Such a reaction is able to synchronize more in structured space and gets more accurate in terms of timing. This property of being able to shorten the reaction time and reduce the noise content can be extremely important from the point of view of biological evolution. A similar situation occurs for o_2, but after local minima are reached both $\nu_\tau(L)$ and $\nu_\sigma(L)$ start increasing. For this organism an optimal choice for $L \approx 4, 5$ exists where reactions are fastest and most accurate. Organism o_3 is another interesting case with $\nu_\tau(L) < 1$ and $\nu_\sigma(L) > 1$. Since the goal is to compare a large number of reactions in such a manner it is impractical to generate the equivalent of figure 3 for every organism studied.

The information provided in figure 3 needs to be compacted further. This is done as follows. Two special values of $D = D_n, D_0$ will be of interest. $L = 0$ with $D = D_0 \gg \xi^\eta\lambda$ ($\eta = 0, 1, -1$) describes a situation when the containers are so close that exchange of chemicals dominates the dynamics. Such a geometry is compact and the norms of vectors $\boldsymbol{\tau}(L)$ and $\boldsymbol{\sigma}(L)$ calculated at $L = 0$ will be denoted by τ_0 and σ_0 respectively. When L is sufficiently large, e.g. $L = 5$, one has network-like geometry with $D = D_n \ll \xi^\eta\lambda$ ($\eta = 0, 1, -1$) and the norms of vectors $\boldsymbol{\tau}(L)$ and $\boldsymbol{\sigma}(L)$ calculated at $L = 5$ will be denoted by τ_n and σ_n respectively. See figure 2 for a way to think about these concepts. To classify each organism in the simplest possible way two quantities will be used: $\nu_\tau = \tau_n/\tau_0$ and $\nu_\sigma = \sigma_n/\sigma_0$. (These correspond to $\nu_\tau(L = 5)$ and $\nu_\sigma(L = 5)$; note the vertical dashed lines in figure 3.)

Figure 4 contains a histogram of all values ν_σ for a large number of organisms (generated by computer). The left pane (panels (a), (c), (e), (g) and (i)) depicts the full $\nu_\sigma \in [0, \infty)$ range, while the right pane (panels (b), (d), (f), (h), and (j)) shows the $\nu_\sigma \in [0, 1]$ range that is mostly interesting. It can be seen from the right pane that there are a large number of organisms (reactions) that draw benefit from running their reactions in structured space in terms of noise reduction. For the organisms depicted in the right pane (not explicitly shown; the vertical mark only indicates their presence) the overall noise content is smaller in network-like geometry than in the compact one (see figure 2).

In terms of noise reduction, the absolute winner is organism o_1 with $\nu_\sigma = 0.019\,01$. The value for $\nu_\tau = 0.030\,52$ is somewhat larger. This indicates that although o_1 draws benefit from being run in network-like geometry by reducing the average reaction time, it draws more benefit in terms of reducing noise content and is, in principle, able to synchronize more in structured space. (Please note that this does not hold initially when L is small; e.g. see figure 3, panel (b), region $0 \leqslant L \leqslant 4$.)

It seems that the statistical properties of reaction time for o_1 are Poisson-like with $\tau(L) \approx \sigma(L)$. Inspection of individual components of $\boldsymbol{\tau}(L)$ and $\boldsymbol{\sigma}(L)$ confirms this, as can be seen from figure 3, panel (a). The variance and average for time needed to achieve individual subtasks closely follow each other. For example, at the point that is used as representative for network-like geometry ($L = 5$, figure 3, panel (a), vertical dashed line) one has $\boldsymbol{\tau}_n = [0.025\,5653] - [0.010\,0074]$, $\boldsymbol{\sigma}_n = [0.015\,3956] - [0.010\,9905]$, $\boldsymbol{\tau}_0 = [0.000\,733\,870] - [0.899\,383]$ and $\boldsymbol{\sigma}_0 = [0.000\,720\,187] - [0.994\,857]$.

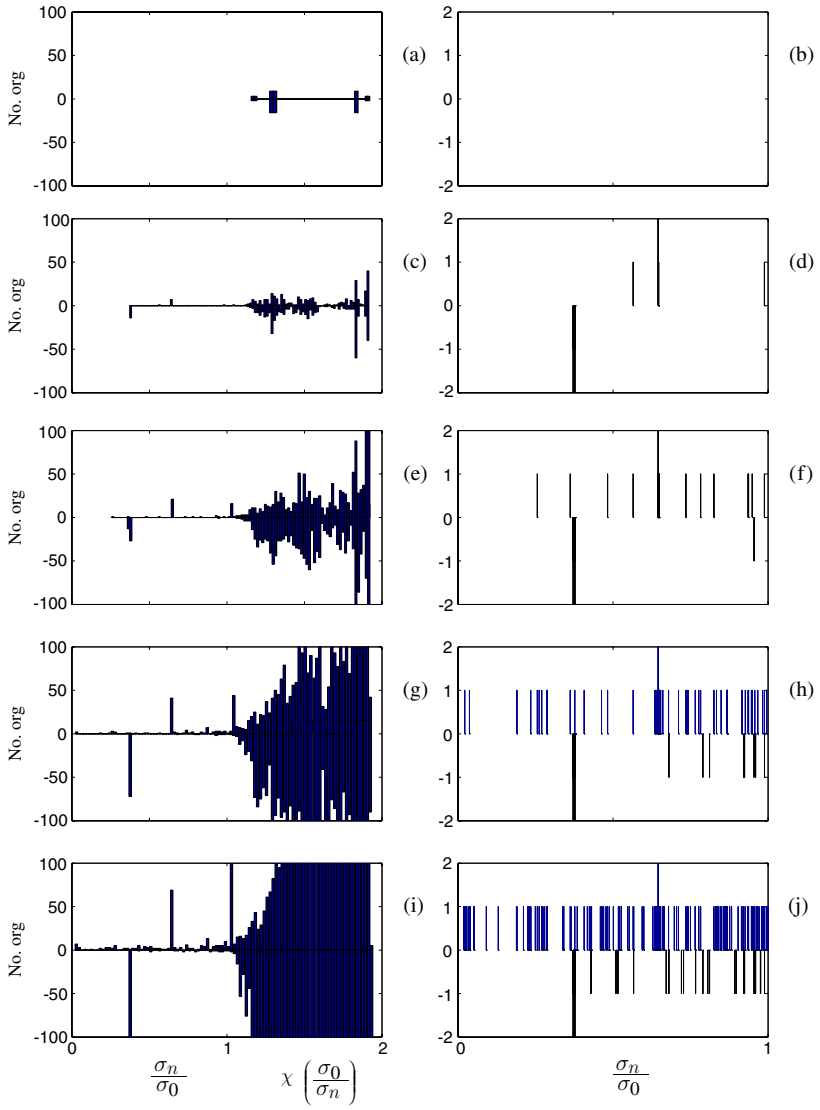

Figure 4. Classification of organisms (calculated with $D_n = 1\ \mathrm{s}^{-1}$, $D_0 = 3125\ \mathrm{s}^{-1}$, $\lambda = 1\ \mathrm{s}^{-1}$, and $\xi = 100$). Panels (a), (c), (e), (g) and (i) are histograms that depict groups with similar values for the ratio $\nu = \sigma_n/\sigma_0$. There are 100 classes of width 0.01 for ν from 1 to 2. The abscissa for values $\nu > 1$ has been rescaled and values obtained from $\chi(\nu) = 2 - \ln 2/\ln(1+\nu)$ are used in the plot. The function χ maps the infinite interval $[1, \infty)$ onto $[1, 2)$ and reveals more detail in the region near $\nu = 1$. Panels (b), (d), (f), (h), and (j) are discrete spectra (no histogram) for the region $\nu \in [0, 1]$. Panels in the same row have same value for the total number of particles in the system N_{p}^*: (a) and (b) $N_{\mathrm{p}}^* = 1$ (95 organisms), (c) and (d) $N_{\mathrm{p}}^* = 2$ (2840 organisms), (e) and (f) $N_{\mathrm{p}}^* = 3$ (3025 organisms), (g) and (h) $N_{\mathrm{p}}^* = 4$ (9560 organisms), (i) and (j) $N_{\mathrm{p}}^* = 5$ (24 890 organisms). A negative value for the number of organisms indicates that the organism with a particular value of ν contains at least one reaction that is inhibited.

(This figure is in colour only in the electronic version)

A very rough understanding of this phenomenon can be gained by inspecting the two-state Markov process, where state (1) is left with rate λ and one arrives in state (2) which

is fully absorbing. In such a case the master equation looks like $\dot{p}_1 = \lambda p_1$, $\dot{p}_2 = -\lambda p_1$. Function $g(t) \equiv \dot{p}_2(t)$ describes the statistics of the reaction time. The Laplace transform of $g(t)$ can be trivially found $G(s) = \lambda/(\lambda + s)$, and it gives $\tau \equiv -G'(0) = 1/\lambda$ and $\sigma^2 \equiv G''(0) - G'(0)^2 = 1/\lambda^2$ leading to $\tau = \sigma$ equality. To some extent the structure of configuration spaces of o_1 very likely resembles the structure of the two-component space just discussed.

There are many organisms that behave in a similar manner having $\nu_\sigma \equiv \sigma_n/\sigma_0 < 1$ and $\nu_\tau \equiv \tau_n/\tau_0 < 1$, but due to lack of space detailed analysis of their features will not be conducted here. On the other hand, it is interesting to discuss cases that behave differently. There are organisms that exhibit heavy non-Poisson behaviour ($\tau \neq \sigma$) having either $\nu_\sigma < 1 < \nu_\tau$ or $\nu_\sigma > 1 > \nu_\tau$. For example, organism o_2 behaves in such a way with $\nu_\sigma = 0.921\,45 < \nu_\tau = 1.1191$. Likewise organism o_3 has $\nu_\sigma = 1.111\,44 > \nu_\tau = 0.840\,83$.

Panel (d) in figure 3 shows an interesting example where both ν_τ and ν_σ can be larger or smaller than one, depending on the distance between containers. Both exhibit minima in the region near $L = 5$. Perhaps, out of o_2 and o_3, the organism o_3 is the best example of a reaction scheme that exhibits non-Poisson statistics since there is a large difference in behaviour of ν_σ and ν_τ (panel (f) in figure 3).

Another interesting feature that can be noted from figure 4 is that there is a range that starts with $\nu_\sigma = 0$ and ends with $\nu_\sigma \approx 0.4$ which is dominated by organisms with only positive (promoter type) catalytic influences (marks indicating the presence of the organism are drawn above the zero line). For example, at total number of particles $N_\mathrm{p}^* = 2$ and at $\nu_\sigma \approx 0.4$ organism o_4 with inhibiting reaction shows up with reaction $A \xrightarrow{-A} B$, $B \xrightarrow{+A} A$ (note the minus sign for the A to B reaction); inject pattern: $\boldsymbol{\iota} = [A] - [B]$; task pattern: $\boldsymbol{\pi} = [2B] - [\ ]$, with $\boldsymbol{\tau}_n = [18.5492] - [\ ]$, $\boldsymbol{\sigma}_n = [19.2581] - [\ ]$, $\boldsymbol{\tau}_0 = [50.9049] - [\ ]$, and $\boldsymbol{\sigma}_0 = [51.8710] - [\ ]$ leading to $\nu_\sigma = 0.371\,269$ and $\nu_\tau = 0.364\,389$. This organism stays as the leading one with the inhibiting reaction scheme in the whole range $N_\mathrm{p}^* = 2, 3, 4, 5$ indicating the existence of a quasi-plateau for these types of organisms. The question is whether increasing N_p^* further would introduce a new organism with similar properties below the current threshold of $\nu_\sigma \approx 0.4$. Unfortunately, due to lack of more powerful computational resources, this question will have to be left open.

5. Conclusions

In this work a special emphasis is placed on issues related to the timing of chemical reactions in structured spaces. The two moments of the reaction time have been analysed, the average $\boldsymbol{\tau}$ and the standard deviation $\boldsymbol{\sigma}$. The average of the reaction time measures the speed of reaction while standard deviations indicate how noisy a reaction is. The special emphasis was on how these quantities change as the reaction volume is altered from compact (open space denoted by '0') towards structured (network-like) with many obstacles present (denoted by 'n').

By changing the value of the jump rate D relative to the reaction rate λ (considering $D = D_0 \gg \lambda$ versus $D = D_n \ll \lambda$) it is possible to study the reaction- and diffusion-controlled regime at the same time (by comparing $\boldsymbol{\tau}_0$ and $\boldsymbol{\sigma}_0$ versus $\boldsymbol{\tau}_n$ and $\boldsymbol{\sigma}_n$) and express a comparison through one parameter ($\nu_\tau \equiv \tau_n/\tau_0$ and $\nu_\sigma \equiv \sigma_n/\sigma_0$).

It has been found that there are reactions that draw simultaneous benefits in terms of increased reaction speed ($\nu_\tau < 1$) and noise reduction ($\nu_\sigma < 1$) by being run in structured spaces. Many reactions (organisms) have Poisson-like statistics which is robust under changes in geometry (going from compact to network-like structure) with $\tau_0 \approx \sigma_0$ and $\tau_n \approx \sigma_n$. Intermediate cases are also possible with strong non-Poisson statistics, where the behaviour

of $\boldsymbol{\tau}$ and $\boldsymbol{\sigma}$ changes asynchronously. For example, when altering the geometry from compact to structured, there are organisms that draw benefit in terms of shorter reaction time but larger noise ($\nu_\tau < 1$ and $\nu_\sigma > 1$), and the other way around ($\nu_\tau > 1$ and $\nu_\sigma < 1$).

The emphasis on the transition from Poisson-like towards non-Poisson-like statistics in this work is not unique. For example, in [38, 39] the impact of energy landscape complexity in various chemical processes (protein folding, or electron transfer) on the reaction time statistics has been studied. Here, the configuration spaces considered are relatively simple (the configuration space is not complex). All variations in the reaction time statistics originate from changes in the system geometry.

A living cell interior is too complicated to be modelled in detail and in this study a simple model of the living cell has been introduced, with a goal to presenting a general platform for studying issues of timing in living cell biochemistry (e.g. by identifying catalytic influences that might make the dynamics sensitive to geometrical changes). In order to make the presentation pedagogical very small systems were studied with only two particle types (A and B) and two containers. The present setup can be easily applied to study more complicated cases. This can be achieved in several ways.

Various technical improvements are possible: for example, by improving the description of transport between containers, or describing chemical reaction dynamics within containers more accurately. Both theoretical and experimental studies are available that deal with these issues [40, 41, 37, 42].

Cases with a larger number of molecule types and containers could be investigated, moving towards an understanding of real chemical reactions in the living cell. There are a couple of studies in which an attempt has been made to model living cells in great detail [43–45]. The present work could be easily extended in a similar direction where whole scale simulations could be merged with the setup presented in this work. In such a way it might be possible to analyse timing issues of concrete processes in the living cell. It would be interesting to extend the findings of this work in this direction, for example by studying the structure of chemical reaction pathways in structures found in the interior of the living cells. A few examples are golgi, mitochondria, and endoplasmic reticulum.

Acknowledgments

The work was supported by a couple of groups at Chalmers University of Technology. For financial support I would like to thank Chalmers Biocenter and other sources: Professor Owe Orwar, Professor Göran Wendin, and Professor Bengt Kasemo. Also, financial help from Adlerbertska forskningsstiftelsen is greatly acknowledged.

References

[1] Calef D F and Deutch J M 1983 *Annu. Rev. Phys. Chem.* **34** 493–524
[2] Rice S A 1985 *Comprehensive Chemical Kinetics* vol 25 *Diffusion-Limited Reactions* (Amsterdam: Elsevier)
[3] Mikhailov A S 1989 *Phys. Rep.* **184** 307–74
[4] Ovcinnikov A A, Timasev S F and Belyi A A 1989 *Kinetics of Diffusion Controlled Chemical Processes* (Commack: Nova Science)
[5] Kotomin E and Kuzovkov V 1992 *Rep. Prog. Phys.* **55** 2079–188
[6] Kotomin E and Kuzovkov V 1996 Modern aspects of diffusion-controlled reactions: cooperative phenomena in bimolecular processes *Comprehensive Chemical Kinetics* vol 34 (Amsterdam: Elsevier)
[7] Privman V 1997 *Nonequilibrium Statistical Mechanics in One Dimension* ed V Privman (Cambridge: Cambridge University Press)

[8] Karlsson M, Davidson M, Karlsson R, Karlsson A, Bergenholtz J, Konkoli Z, Jesorka A, Lobovkina T, Hurtig J, Voinova M and Orwar O 2004 *Annu. Rev. Phys. Chem.* **55** 613–49
[9] Mcquarrie D A, Russell M E and Jachimowicz C J 1964 *J. Chem. Phys.* **40** 2914
[10] McQuarrie D 1967 *J. Appl. Probab.* **4** 413
[11] Tachiya M 1980 *Chem. Phys. Lett.* **69** 605–7
[12] Rothenberger G, Infelta P P and Gratzel M 1981 *J. Phys. Chem.* **85** 1850–6
[13] Clifford P, Green N J B and Pilling M J 1982 *J. Phys. Chem.* **86** 1318–21
[14] Clifford P, Green N J B and Pilling M J 1982 *J. Phys. Chem.* **86** 1322–7
[15] Ramamurthy V 1991 *Photochemistry in Organized and Constrained Media* (New York: VCH)
[16] Khairutdinov R F and Serpone N 1996 *Prog. React. Kinetics* **21** 1–68
[17] Khairutdinov R F, Burshtein K Y and Serpone N 1996 *J. Photochem. Photobiol.* A **98** 1–14
[18] Berberan-Santos M N, Bodunov E N and Martinho J M G 1998 *Opt. Spectrosc.* **85** 869–72
[19] Stange P, Zanette D, Mikhailov A and Hess B 1999 *Biophys. Chem.* **79** 233–47
[20] Nelsestuen G L 1999 *Chem. Phys. Lipids* **101** 37
[21] Luby-Phelps K 2000 *Int. Rev. Cytol.* **192** 189–221
[22] Pagliaro L 2000 *Int. Rev. Cytol.* **192** 303–18
[23] Kuthan H 2001 *Prog. Biophys. Mol. Biol.* **75** 1
[24] Stryer L 1992 *Biochemistry* (New York: Freeman)
[25] Mikhailov A and Hess B 1996 *J. Phys. Chem.* **100** 19059–65
[26] Stange P, Mikhailov A S and Hess B 1998 *J. Phys. Chem.* B **102** 6273–89
[27] Stange P, Mikhailov A S and Hess B 1999 *J. Phys. Chem.* B **103** 6111–20
[28] Stange P, Mikhailov A S and Hess B 2000 *J. Phys. Chem.* B **104** 1844–53
[29] Qian H and Qian M 2000 *Phys. Rev. Lett.* **84** 2271–4
[30] Kai S and Qi O Y 2001 *Phys. Rev.* E **6402** 026111
[31] Wang H L, Qi O Y and Lei Y A 2001 *J. Phys. Chem.* B **105** 7099–103
[32] Konkoli Z 2005 *Phys. Rev.* E **72** 011917
[33] Mannella C A 2000 *J. Bioenerg. Biomembr.* **32** 1–4
[34] Mannella C A, Pfeiffer D R, Bradshaw P C, Moraru I, Slepchenko B, Loew L M, Hsieh C, Buttle K and Marko M 2001 *Iubmb Life* **52** 93–100
[35] Mannella C A 2006 *Biochim. Biophys. Acta* **1762** 140–7
[36] Karlsson A, Karlsson R, Karlsson M, Cans A S, Stromberg A, Ryttsen F and Orwar O 2001 *Nature* **409** 150–2
[37] Lizana L and Konkoli Z 2005 *Phys. Rev.* E **72** 026302
[38] Wang J and Wolynes P 1999 *J. Chem. Phys.* **110** 4812–9
[39] Wang J and Wolynes P 1995 *Phys. Rev. Lett.* **74** 4317–20
[40] Konkoli Z, Karlsson A and Orwar O 2003 *J. Phys. Chem.* B **107** 14077–86
[41] Karlsson A, Sott K, Markstrom M, Davidson M, Konkoli Z and Orwar O 2005 *J. Phys. Chem.* B **109** 1609–17
[42] Sott K, Lobovkina T, Lizana L, Tokarz M, Bauer B, Konkoli Z and Orwar O 2006 *Nano Lett.* **6** 209–14
[43] Schaff J, Fink C C, Slepchenko B, Carson J H and Loew L M 1997 *Biophys. J.* **73** 1135–46
[44] Schaff J C, Slepchenko B M, Choi Y S, Wagner J, Resasco D and Loew L M 2001 *Chaos* **11** 115–31
[45] Tomita M 2001 *Trends Biotechnol.* **19** 205–10